Pirfenidone normalizes the tumor microenvironment to improve chemotherapy

Supplementary Materials

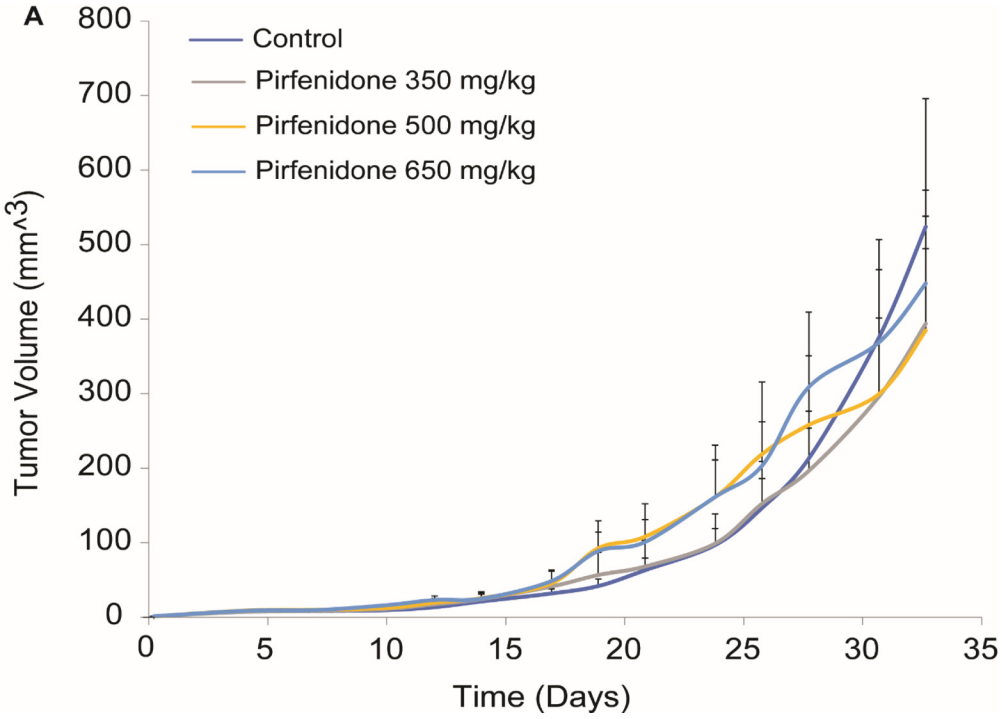

Supplementary Figure 1: Pirfenidone does not affect tumor volume growth rates. Tumor volume growth rates of orthotopic MCF10CA1a human breast tumors implanted in female CD1 nude mice. Pirfenidone-treated mice alone show no significantly effect on tumor volume.

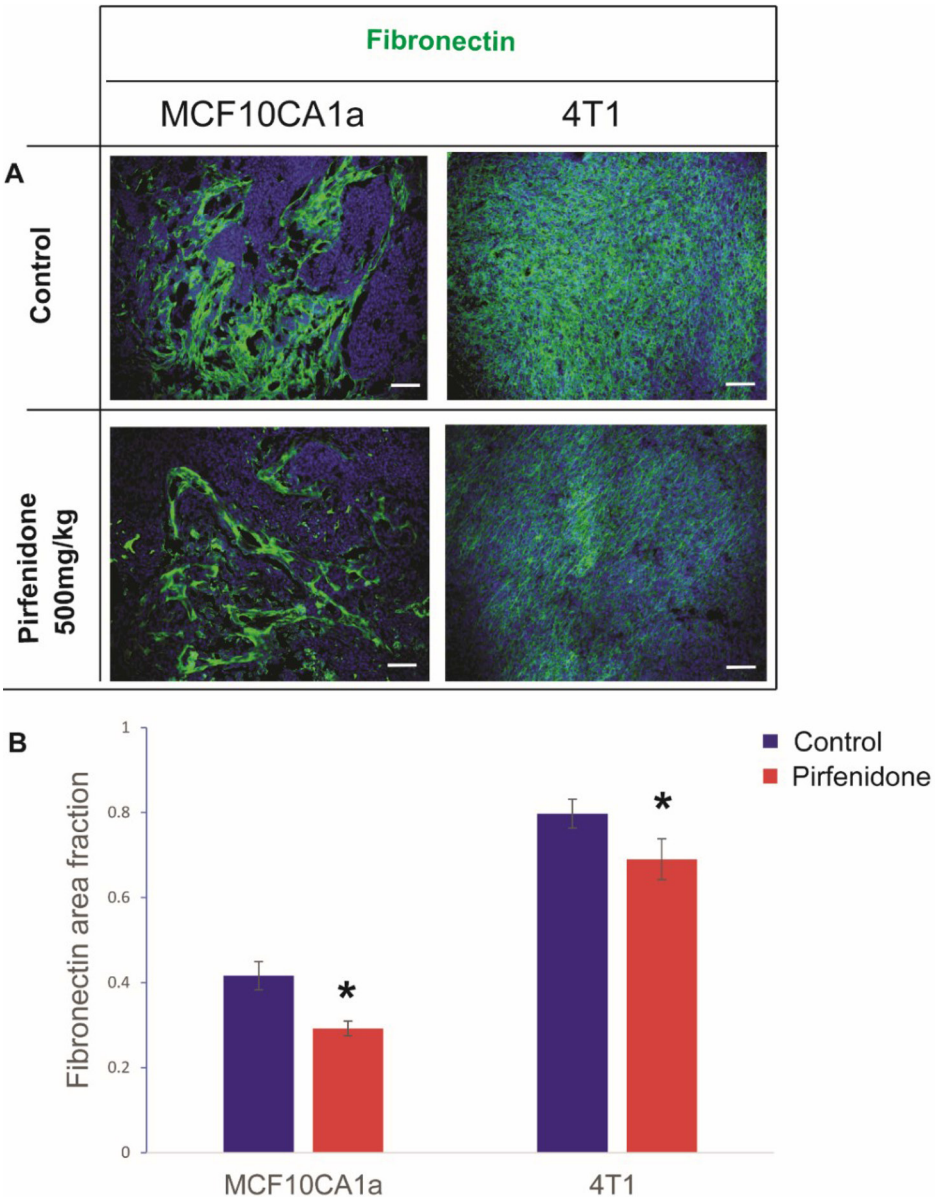

Supplementary Figure 2: Pirfenidone reduces fibronectin expression in MCF10CA1a and 4T1 breast tumors. (**A**) Representative immunofluorescent images from histological analysis for MCF10A1a and 4T1 control and Pirfenidone-treated tumors show the effect of Pirfenidone on Fibronectin expression. (**B**) Quantification of area fraction of fibronectin indicates that its expression level is significantly reduced compared to control tumors. Asterisks indicate statistically significant difference between groups ($p < 0.05$). Scale bar: 100 μm.

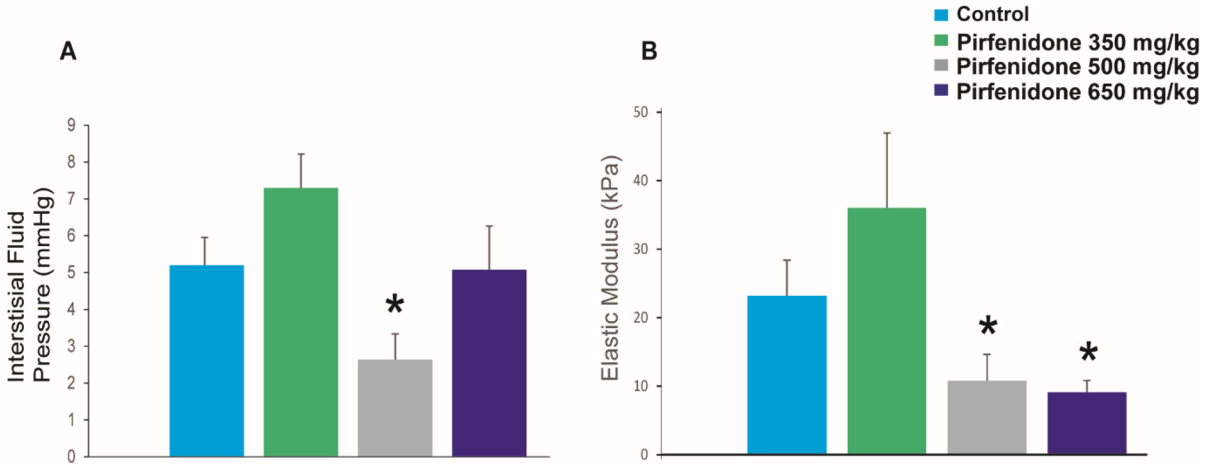

Supplementary Figure 3: Mechanical properties of Pirfenidone-treated MCF10CA1a breast tumors. (**A**) The values of the Interstitial Fluid Pressure (IFP) for the Pirfenidone-treated tumors are shown to be significantly lower at 500 mg/kg compared to control as well as to those of 350 mg/kg and 650 mg/kg Pirfenidone-treated MCF10CA1a breast tumors. (**B**) The values of the elastic modulus for the 500 mg/kg and 650 mg/kg Pirfenidone-treated tumors are shown to be significantly lower compared to those of control and 350 mg/kg Pirfenidone-treated MCF10CA1a breast tumors (* indicates p value < 0.05).

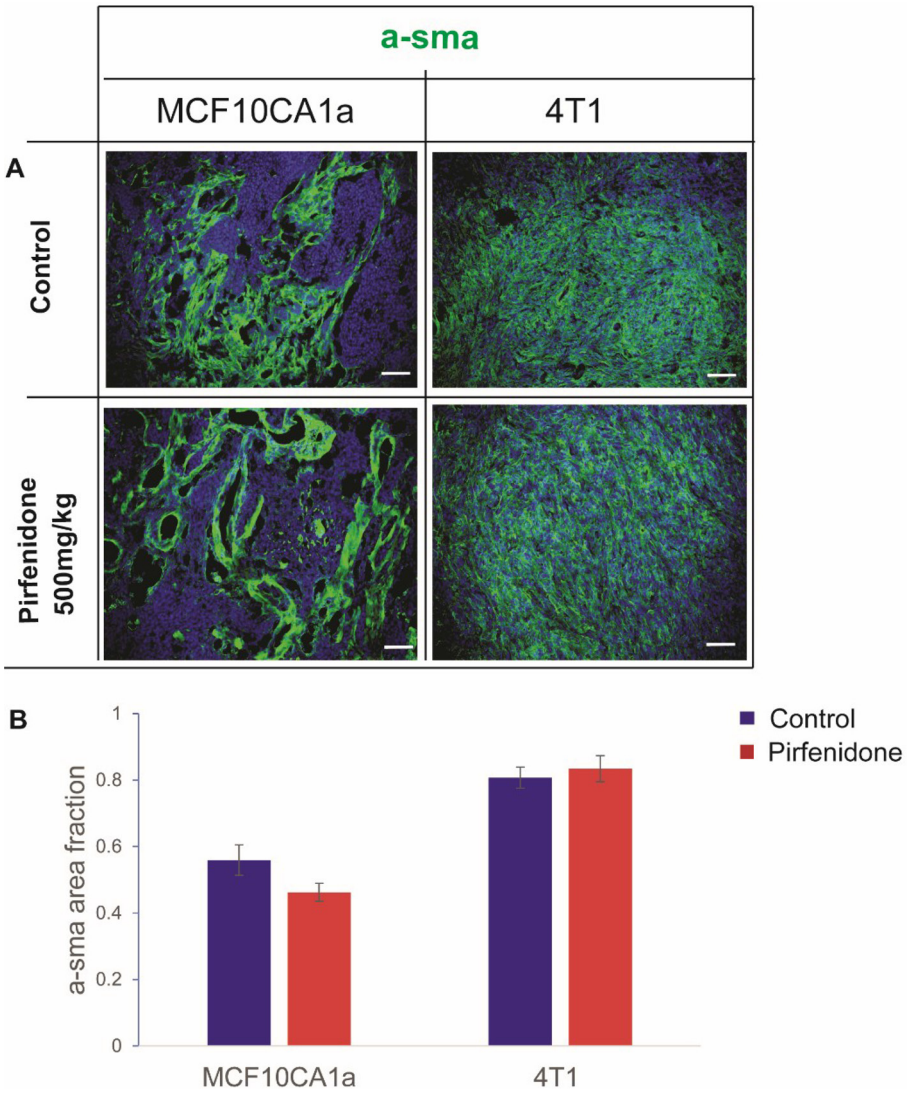

Supplementary Figure 4: Pirfenidone does not affect alpha smooth muscle actin (a-sma) expression in MCF10CA1a and 4T1 breast tumors. (**A**) Representative immunofluorescent images of control and Pirfenidone-treated MCF10CA1a and 4T1 tumors for a-sma. (**B**) Area fraction analysis shows no statistically significant difference between compared groups indicating that Pirfenidone has no effect on the expression of a-sma in both breast tumor models. Scale bar: 100 μm.

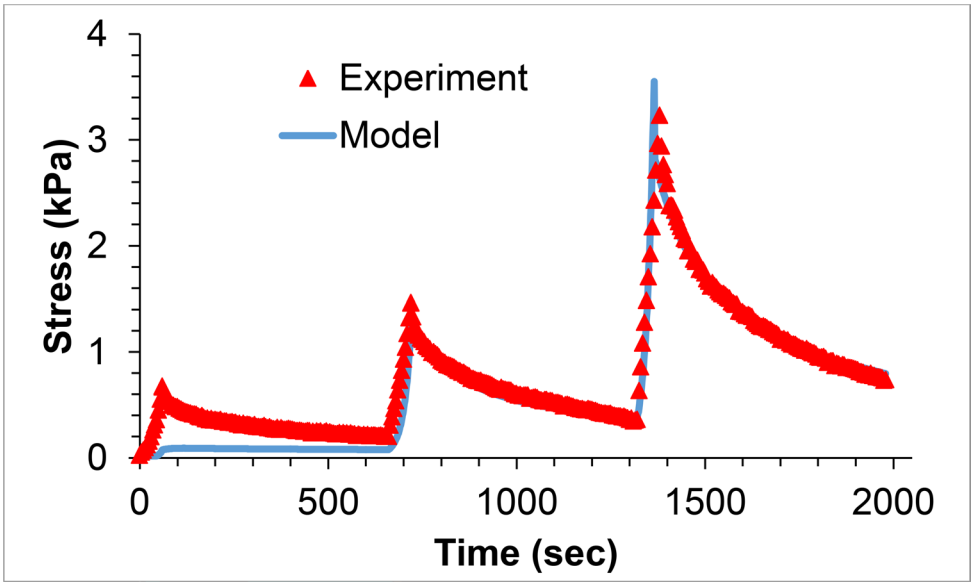

Supplementary Figure 5: Calculation of the hydraulic conductivity of the tumor. Representative stress relaxation data of the tumors that were tested along with the fit of a biphasic model [3]. The hydraulic conductivity was calculated by fitting the biphasic model to the experimental data.

Supplementary Table 1: Human-specific primers that were used for gene expression analysis of cancer cells from MCF10CA1a breast tumors

Gene	Primer sequence
hCOL1A1 F	GTGCTAAAGGTGCCAATGGT
hCOL1A1 R	ACCAGGTTCACCGCTGTTAC
hHAS1 F	TCGGAGATTCGGTGGACTAC
hHAS1 R	GTCCAACCTTGTGTCCGAGT
hHAS2 F	ACCGGGGTAAAATTTGGAAC
hHAS2 R	TAAGGCAGCTGGCAAAAGAT
hHAS3 F	TTTGCCATTGCTACCATCAA
hHAS3 R	AGGCCAATGAAGTTCACCAC
hB-ACTIN F	CGAGCACAGAGCCTCGCCTTTGCC
hB-ACTIN R	TGTCGACGACGAGCGCGGCGATAT
hFN1 F	GATGCTCCCACTAACCTCCA
hFN1 R	CGGTCAGTCGGTATCCTGTT
hPOSTN F	TTCTGACGCCTCAAAACTGA
hPOSTN R	TGCTCTCCAAACCTCTACGG
hVIM F	CGAAAACACCCTGCAATCTT
hVIM R	ATTCCACTTTGCGTTCAAGG
hCOL3 F	TAGGTCCATCTGGTCCTGCT
hCOL3 R	CGAAGCCTCTGTGTCCTTTC
hCOL4 F	CTCTACGTGCAAGGCAATGA
hCOL4 R	AGAACAGGAAGGGCATTGTG
hLOX F	CAGAGGAGAGTGGCTGAAGG
hLOX R	CCAGGACTCAATCCCTGTGT
hTGF-B1 F	GTACCTGAACCCGTGTTGCT
hTGF-B1 R	CACGTGCTGCTCCACTTTTA

SUPPLEMENTARY MATERIALS AND METHODS

Pirfenidone normalizes the tumor microenvironment to improve chemotherapy

Fluorescent immunohistochemistry and vessel perfusion histology

MCF10CA1a and 4T1 breast tumors were excised from mice, fixed and embedded in optimal cutting temperature compound (OCT). Transverse 40 μm-thick tumor sections were produced using the Tissue-Tek Cryo3 (SAKURA) and immunostained with antibodies against collagen I (ab4710, Abcam 1:100 dilution), CD31 (MEC13.3, BD Biosciences, 1:100 dilution) hyaluronan (ab53842, Abcam 1:100 dilution), fibronectin (Hybridoma, 1:50 dilution) and a- smooth muscle actin (ab5694, Abcam, 1:100) counterstained with 4′,6-diamidino-2-phenylindole (Vector Labs). Antigens were detected using appropriate secondary fluorescent antibodies. Collagen I was detected with Alexa Fluor-647 Goat Anti-Rabbit IgG (H+L) secondary antibody (A-21244, Invitrogen, 1:800 dilution), CD31 with Alexa Fluor-647 Goat Anti-Rat IgG (H+L) secondary antibody (A-21247, Invitrogen, 1:800 dilution), and hyaluronan using Alexa Fluor-647 donkey Anti-sheep IgG (H+L) secondary antibody (A-11015, 1:800 dilution). For blood vessel perfusion analysis, mice were slowly injected with 100 μl of 1 mg/ml biotinylated lycopersicon esculentum (tomato) lectin (Vector Labs) *via* intracardiac injection 7 minutes prior to euthanization and tumor removal. Upon excision, tumors were fixed in paraformaldehyde, embedded in OCT and frozen. Transverse 40 μm-thick tumor sections were produced and stained with an antibody against the endothelial marker CD31. Streptavidin-conjugated and fluorescently-labelled secondary antibodies against lectin and CD31 were used to detect these antigens, respectively. Lectin staining was detected using the Streptavidin Alexa Fluor 488 conjugate (Molecular probes, S11223, 1:400 dilution) and CD31 signal was detected with Alexa Fluor-647 Goat Anti-Rat IgG (H+L) secondary antibody (Molecular probes, A-21247, 1:800 dilution). Images from anti-collagen I, anti-CD31, anti-hyaluronan and anti-biotin-stained sections were analysed based on the area fraction of positive staining. To avoid any bias, the analysis was performed automatically using a previously developed in-house code in MATLAB (MathWorks, Inc., Natick, MA, USA) [1]. Vessel diameter was calculated from the CD31 images. Specifically, the procedure of the identification of the non-collapsed vessels was automated in the MATLAB code. The CD31 staining that forms a loop was considered to be a vessel and the short axis of a cross-section fit to an oval was taken. Five different sections per tumor (from the interior and the periphery) at ×10 magnification were taken and analyzed keeping the analysis settings and thresholds the same for all tumors.

Biodistribution analysis

For the biodistribution study, a dose of 9 mg/kg of doxorubicin was injected via tail vein injection to the animals and 4 hours post injection they were sacrificed. Six animals per group were tested (n = 6). The tissues were excised from the mice and were stored at −80°C until extraction. For doxorubicin extraction, we used a previously described method with modifications [2]. The tissue samples were homogenized by using a homogenizer in 4 parts (v/w) cell lysis buffer (RIPA buffer). Then in 200 μl of the homogenate were added 50 μl 10% Triton X-100 and 750 μl 0.75N hydrochloric acid (HCl) in isopropanol. The mixture was well-vortexed and let overnight at -20oC for doxorubicin extraction. Samples were again vortexed at RT followed by centrifugation for 30 min at 4°C (14000 rpm). The supernatant was then collected from all samples and fluorescence was measured (Ex.: 470 nm, Em: 590 nm) using the Qubit 3.0 Fluorometer (Life Technologies). A standard curve was established by adding known amounts of doxorubicin to homogenates of non-treated tissue samples prior to extraction.

REFERENCES

1. Stylianopoulos T, Martin JD, Chauhan VP, Jain SR, Diop-Frimpong B, Bardeesy N, Smith BL, Ferrone CR, Hornicek FJ, Boucher Y, Munn LL, Jain RK. Causes, consequences, and remedies for growth-induced solid stress in murine and human tumors. Proc Natl Acad Sci USA. 2012; 109:15101–15108.
2. Laginha KM, Verwoert S, Charrois GJ, Allen TM. Determination of doxorubicin levels in whole tumor and tumor nuclei in murine breast cancer tumors. Clin Cancer Res. 2005; 11:6944–6949.
3. Angeli S, Stylianopoulos T. Biphasic modeling of brain tumor biomechanics and response to radiation treatment. J Biomech. 2016; 49:1524–1531.